Energy Conversion and Management: X 10 (2021) 100071

Contents lists available at ScienceDirect

Energy Conversion and Management: X

journal homepage: www.sciencedirect.com/journal/energy-conversion-and-management-x

Fast pyrolysis kinetics of lignocellulosic biomass of varying compositions

Deepak Kumar Ojha [a,b,*], Daniel Viju [b], R. Vinu [b]

[a] Department of Chemical Engineering, Indian Institute of Technology Roorkee, Roorkee 247667, India
[b] Department of Chemical Engineering and National Center for Combustion Research and Development, Indian Institute of Technology Madras, Chennai 600036, India

ARTICLE INFO

Keywords:
Rice straw
Empty fruit bunch
Pine wood
Fast pyrolysis
Py-FTIR
Py-GC/MS
Kinetics

ABSTRACT

This study is focused on evaluating the apparent kinetics of fast pyrolysis of different lignocellulosic biomass *viz,* rice straw, pine wood and empty fruit bunch. The goal of the study is to investigate the effect of biomass composition on kinetics, time evolution of pyrolysis vapors and the production of major bio-oil components during the fast pyrolysis of biomass. The isothermal mass loss data were generated at different pyrolysis times between two and sixty seconds in the temperature range of 400–700 °C. The data generated were then analyzed using various reaction models, *viz.*, first-order model, diffusion models, contracting cylinder model and Avrami-Erofeev model to determine the rate constants and the rate parameters. Kinetic compensation effect was established using a large number of kinetic data reported in the literature to validate the results. The time evolution of major functional groups in the pyrolysates was analyzed using *in-situ* analytical pyrolyzer coupled with Fourier transform infrared spectrometer (Py-FTIR), and evolution of the volatiles was observed in time range of 5–60 s. Increase in pyrolysis temperature led to faster evolution of volatiles as evidenced by the shifting of maximum rate of vapor evolution to shorter time periods.

1. Introduction

Lignocellulosic biomass is regarded as the third largest energy source after coal and petroleum products, and one of the major sources of renewable carbon. Its wide availability across the world makes it one of the most suitable candidates for the production of chemicals and fuel intermediates. Various techniques exist based on biological (fermentation, enzymatic), chemical (solvolysis) and thermochemical (pyrolysis, gasification, liquifaction) routes to convert the lignocellulosic biomass into bio-fuels and chemicals [1,2]. However, among the existing technologies, thermochemical processes such as fast pyrolysis and gassification are highly preferred due to shorter processing time and value of products obtained from them. Fast pyrolysis involves heating of biomass at very high heating rates (>1000 °C/s) to moderate temperatures (400–700 °C) in inert atmosphere. It yields *c.a.* 70% liquid product known as 'pyrolysis oil' (organics + water) besides solid (char + coke) and gaseous products [3]. The overall energy density of the pyrolysis-oil is expected to be four to seven times the overall energy density of biomass [4]. The pyrolysis-oil is a complex mixture of various oxygenates such as aldehyde/ketone, carboxylic acids, furan and pyran derivatives, anhydrosugars and phenol derivatives [5,6]. Due to high oxygen content, the pyrolysis-oil is highly unstable, highly acidic and possesses lower calorific value as compared to petroleum crude oil. The quality of the pyrolysis oil is largely dependent on the genotype of the biomass and pyrolysis conditions [7,8]. However, the presence of heterogeneous non-biological impurities such as ash and minerals could play a key role in the progression of the process, and the yield of various products [9].

Ideally, the time scale of fast pyrolysis is known to be of the order of few seconds. However, in real situations, where the heat and mass transport limitations are non-negligible, it takes a longer time to completely pyrolyze the sample and sweep out the vapors. The time scale of fast pyrolysis is well visualized by Krumm et al.[10] and later by Maduskar et al.[11] using pulse-heated analysis of solid reactions (PHASR) technique. Their analysis demonstrated that the pyrolysis reaction could complete well within 1000 ms. The study by Maduskar et al. also highlighted that the critical characteristic length should be lesser than 10 μm to operate the pyrolysis in isothermal, reaction controlled regime. Through a microkinetic model, Vinu and Broadbelt [12] predicted that a complete conversion of cellulose at 500 °C can be achieved within 1000 ms. The finding of these studies are vital in understanding the progression of pyrolysis at different temperatures. However, it is limited to cellulose samples of a very small size in near-reaction controlled regime. The findings can not be extended to the cases

* Corresponding author at: Department of Chemical Engineering, Indian Institute of Technology Roorkee, Roorkee 247667, India.
E-mail address: dojha@ch.iitr.ac.in (D.K. Ojha).

https://doi.org/10.1016/j.ecmx.2020.100071
Received 6 October 2020; Accepted 23 December 2020
Available online 30 December 2020

where cellulose of larger particle sizes are used, or where lignocellulosic biomass is used instead of cellulose. In our previous studies, we estimated the time scale of product evolution in the fast pyrolysis of alkali lignin using analytical pyrolyzer coupled with Fourier transform infrared spectrometer (Py-FTIR). The study estimated the product evolution time of the order of few minutes [13].

Thermogravimetric analyzer (TGA) alone or coupled with FTIR spectrometer (TGA-FTIR) is exclusively used to understand the gas or solid phase reaction kinetics at slow heating rates (<100 °Cmin^{-1}), by identifying and monitoring the time evolution of various products [14-18]. In one such study, the interaction among the three biomass components, viz., cellulose, hemicellulose, and lignin, were investigated by *Liu et al* [17]. The study concluded that there is a strong interaction between lignin and hemicellulose in a biomass at low temperatures (<327 °C), and between hemicellulose and cellulose at higher temperatures (>327 °C). Additionally, the presence of lignin is shown to affect the yield of key products such as 2-furaldehyde and carbonyl-containing components. In another TGA-FTIR study, catalytic effect of activated charcoal on biomass pyrolysis was investigated in different temperature and composition ranges [18]. The study revealed great details about temporal vapor evolution and time scale of pyrolysis. However, these studies have certain limitations. Firstly, these studies are carried out at low heating rates (5–100 °Cmin^{-1}) and hence can not be fairly extrapolated to fast pyrolysis conditions. There were efforts by various researchers to study the kinetics at higher heating rates. In one of such efforts, Ojha et al. [13,19,20] estimated the kinetic parameters for fast pyrolysis of lignin. By using analytical pyrolyzer coupled with FTIR (Py-FTIR), they also identified the interactions between cellulose and polypropylene at very high heating rate (>200 °C/s). They observed a reduction in pyrolysis time scale when polypropylene was co-fed with cellulose [19,20].

The apparent activation energy and pre-exponential factor for biomass pyrolysis are primarily calculated using mass loss data generated over a range of heating rates using TGA. In a typical analysis, the mass loss data are fitted to model-free isoconversional models of Friedman, Kissinger-Akahira-Sunose (KAS), or Ozawa-Flyn-Wall [21-24] to determine the activation energy and pre-exponential factor. The isoconversional models are very simple to use and it utilizes temperature *vs* conversion data generated at multiple linear heating rates. The main shortcoming of the linear heating rate experiment is that it fails to identify the acceleratory and sigmoidal regimes. However, it can be identified by utilizing the combination of isothermal and linear heating rate experiments [21]. *Mishra and Bhaskar* [25] determined the activation energy for rice straw as 155.8 kJ/mol and 236.7 kJ/mol in the conversion ranges of 5–60% and 61–90%, respectively, using model-free kinetic methods. In another study based on isothermal data at 265 °C, a relatively low activation energy of 116 kJ/mol is reported for rice straw pyrolysis [26]. The activation energy of pine wood pyrolysis was estimated using distributed activation energy model (DAEM) as 165 kJ/mol [27]. It is important to note that the kinetic parameters calculated at lower heating rates may not be valid at fast heating rate conditions. This means reliable data of weight loss profile at high heating rate is required to estimate the kinetics of fast pyrolysis.

The current study is intended to investigate the kinetics of fast pyrolysis of three lignocellulosic biomass, viz. rice straw (RS), pinewood (PW) and empty fruit bunch (EFB). The study has three major parts. In the first part, the isothermal mass loss profiles under fast pyrolysis conditions were generated using the analytical Pyroprobe® reactor. Subsequently, the mass loss data were used to estimate the apparent kinetic parameters such as activation energy and pre-exponential factor. A kinetic compensation plot is generated using the existing literature data to validate the obtained kinetic parameters. In the second part, the time scale of the fast pyrolysis of biomass is estimated using Py-FTIR. In the third part, the fast pyrolysis products from RS, PW and EFB were identified using analytical pyrolyzer coupled with gas chromatograph/mass spectrometer (Py-GCMS).

2. Materials and methods

2.1. Materials

Three agro residues, viz. EFB, PW, and RS, were selected on the basis of difference in composition and ash content. The detailed composition of these biomasses are presented in Table 1 and Table 2. These biomass samples were obtained from Valmet Technologies, Chennai. The materials were crushed using a domestic grinder, and particles in the size range 0.30–0.50 mm were obtained by sieving.

The proximate analysis, ultimate analysis and higher heating value (HHV) of the biomass were performed according to the American Society for Testing and Materials (ASTM) guidelines, and are depicted in Table 1. It is clear that RS contains highest ash (18.9%) among the three biomass followed by the EFB (7.5%) and PW (0.7%). PW contains highest volatile matter (74.8%) but it also contains high fixed carbon (~17%). The results of the proximate and elemental analyses are found to be in agreement with the literature [28].

2.2. Isothermal mass loss of biomass and Py-FTIR analysis

The isothermal mass loss profiles of biomass under fast pyrolysis conditions were generated in a Pyroprobe® 5150 pyrolyzer (CDS Analytical, U.S.A.) integrated with a stainless-steel Brill cell. The snapshot of the Brill cell is depicted in Fig. S1 (Supplementary Information). The Brill cell consists of two Zinc-selonide (ZnSe) windows on two sides to facilitate the IR scanning of the pyrolysis vapors. The Brill cell was placed in the beam path of an FT-IR spectrometer (Agilent Cary 660 series) to monitor the pyrolysis vapors. However, for mass loss experiments, FTIR spectrometer was not turned on. In a typical mass loss experiment, 8 ± 0.2 mg of pre-dried biomass was measured using high precision microbalance (Sartorius Cubis, ±1 μg accuracy). The biomass was loaded in the quartz tube and packed with a glass wool on both ends. The quartz tube was placed inside the resistively heated Pt-filament coil, which was then placed inside the Brill cell. Nitrogen gas was continuously purged through the Brill cell at 110 mL min^{-1}, which was held at 200 °C to avoid any vapor condensation. The temperature and flow rate were optimized in such a way that the vapors do not condense on the ZnSe windows. Before starting the experiment, the Brill cell was was purged with N_2 for 10 min to establish inert atmosphere.

In order to obtain the mass loss profiles, the biomass sample was heated to various temperatures and maintained at different hold times. The different hold times used were 2, 4, 6, 8, 10, 15, 20, 30 and 60 s and the temperatures were 400, 450, 500, 550, 600, 650 and 700 °C. At the end of the experiment, the mass of the biomass remaining in the quartz tube was measured using a microbalance. Each experiment was repeated at least three times to check the repetability, and the standard error is reported.

In order to obtain the time evolution of functional groups of the pyrolysates, the FTIR spectrometer was turned on. The FTIR was

Table 1
Detailed characterization of three biomass as used in fast pyrolysis experiments.

	RS	PW	EFB
Proximate Analysis (air dried basis)			
Moisture (wt.%)	8.8	7.7	9.8
Volatile (wt.%)	63.8	74.8	66.1
Fixed carbon (wt.%)	8.5	16.8	16.6
Ash (wt.%)	18.9	0.7	7.5
Ultimate Analysis (dry basis)			
C (wt.%)	38.0	47.1	38.3
H (wt.%)	5.5	6.2	5.1
N (wt.%)	0.8	0.1	1.2
O (wt.%)*	36.8	45.9	47.7
S (wt.%)	0.0	0.0	0.2
HHV (MJ/kg)	14.7	20.4	15.9

*O = 100 – C – H – N – S – Ash.

Table 2
Composition of ash (in wt.%) extracted from EFB, PW and RS [28].

Metal oxides	Composition in ash (%)		
	EFB	PW	RS
SiO_2	63.20	9.71	77.20
Al_2O_3	4.50	2.34	0.55
Fe_2O_3	3.90	2.10	0.50
SO_3	2.80	2.22	1.18
CaO	9.0	48.88	2.46
MgO	3.80	13.80	2.71
Na_2O	0.80	0.35	1.79
K_2O	9.0	14.38	12.59
P_2O_5	2.80	6.08	0.98
TiO_2	0.20	0.14	0.04

equipped with a linear, highly sensitive mercury-cadmium-telluride (MCT) detector. The FTIR is set to aquire three spectra every second in the scan range of 4000–600 cm^{-1} at a resolution of 2 cm^{-1}. The total scan time was set to 60 s. The time-based spectra were generated based on Gram-Schmidt function [29].

2.3. Product analysis using Py-GC/MS

Fast pyrolysis experiments were carried out in Pyroprobe® 5200 pyrolyzer (CDS Analytical, U.S.A.) interfaced with gas chromatograph/mass spectrometer (GC/MS, Agilent Technologies, model 7890-5975C). In a typical experiment, 500 ± 50 μg sample was packed inside the Pt-coil filament as described earlier. The sample was then pyrolyzed at desired temperatures (400, 500, 650, 800 °C) and held for 30 seconds. The vapors generated during pyrolysis were continuously passed through an online Tenax® trap, where it gets adsorbed. After the completion of pyrolysis, the temperature of the Tenax® cartridge was increased to 300 °C in 3 min to quickly desorb the vapors. Subsequently, the desorbed vapors were passed through he GC/MS for product analysis.

The transfer line was connected to the GC injector which was set at 280 °C. The incoming pyrolysis vapors were separated using HP-5 ms (30 m × 0.25 mm i.d. × 0.25 μm film thickness) capillary column. The GC column oven was initially held at 40 °C for 2 min, followed by a ramp of 10 °C min^{-1} to 280 °C, and finally held at this temperature for 2 min. Ultra-high pure helium (99.9995%) was used a carrier gas for GC/MS. The carrier gas flow rate was set at 1 mL min^{-1}. The separated analyte from the GC was transferd to the MS using a GC/MS interface. The GC/MS interface and ion source temperatures were maintained at 300 °C and 250 °C, respectively. The incoming pyrolysates were scanned in the mass range (m/z) of 28–400 Da at an electron ionization voltage of 70 eV. The mass spectra of the pyrolysates were compared with NIST and Biofuel libraries, and the compounds that had a match-factor>80% were considered. The relative composition of the pyrolysates is reported in terms of GC/MS peak area%.

3. Result and discussions

3.1. Kinetics of the fast pyrolysis of biomass

The fundamental equation to describe the the rate of conversion of the sample is given by [21]

$$\frac{d\alpha}{dt} = k(T)f(\alpha)$$

where α is mass conversion with time t, and k(T) is described by Arrhenius equation. The function f(α) describes the dependence of conversion on the progress of the reaction. The equation can be integrated for isothermal condition to yield,

$$g(\alpha) = \int_0^{\alpha} \frac{d\alpha}{f(\alpha)} = Ae^{\frac{-E}{RT}} \int_0^{t} dt = k(T)\cdot t$$

Where A (also denoted as k_0), E and R denote pre-exponential factor, apparent activation energy and universal gas constant, respectively. The function g(α) is derived for various models in the literature, and given in Table 3.

The isothermal mass loss profiles of RS, EFB, and PW, generated under fast pyrolysis conditions, are depicted in Fig. 1. It is important to note that each data point in the mass loss profile corresponds to an experiment performed at a specific temperature and hold time. It is evident that different biomass samples behave differently when exposed to same temperature and hold time, i.e. the mass of different biomass samples decreases at different rates at similar experimental conditions. To understand better, if we consider a temperature of 400 °C and holding time of 30 s, the remaining sample mass is observed as 63%, 42%, and 41%, for PW, EFB, and RS, respectively. The dependence of rate of thermal degradation on the bio-chemical composition of biomass, i.e. cellulose, hemicellulose, lignin, and ash content is well established [30]. The bio-chemical composition of the EFB, PW, and RS, are reported in the literature, are given in the Table 4 [31-33].

Typically, the degradation of cellulose and hemicellulose starts at a lower temperature (~200 °C) and completes well within 500 °C, while, lignin degrades in a wide temperature range of 400–800 °C [34]. Overall, the high temperature degradation of biomass is attributed to the lignin content and the secondary reaction of lignin-derived products with char. The lignin content can be qualitatively related to the fixed carbon in the biomass; higher fixed carbon content in the biomass is indicative of higher lignin content [35]. It is worth mentioning that, pine wood and empty oil palm fruit bunch are derived from woody biomass source, and these show a relatively higher fixed carbon or lignin content in comparison with rice straw, which is basically a harvested agro residue.

The rate constants obtained for fast pyrolysis of EFB, PW and RS at different temperatures according to various models are presented in Tables S1-S3 (Supplementary Information). The linear regression of the above mentioned models at different temperatures are depicted in Figures S2-S19 (Supplementary information). All the linear fits were generated with a minimum of five data points.

In order to identify the model that best describes the fast pyrolysis kinetics of biomass, the regression coefficients of different models were compared. It is observed that the decelerating models such as diffusion models exhibit a reasonable regression coefficient of $R^2 > 0.90$ for all the biomass samples (Tables S1-S3). However, low regression coefficient values (0.9–0.95) are observed at high temperatures. The apparent activation energies (Table 5) vary in the range of 34–40 kJ/mol, 35–50 kJ/mol and 13–29 kJ/mol for EFB, PW, and RS, respectively. It is interesting to note that the activation energy values obtained in this study are much lower than the previously reported values. This can be attributed to the decomposion process being diffusion controlled. The kinetic falsification due to mass transfer, especially internal diffusion limitations are well established and the true activation energy is always estimated to be twice of the apparent activation energy [36]. The lower apparent activation energy of fast pyrolysis for rice straw indicates that

Table 3
Details of various models used in this study to obtain the kinetic parameters [21].

Sl. No.	Model	f(α)	g(α)
1	First Order	(1-α)	−ln(1-α)
2	1D-Diffusion	1/(2α)	α^2
3	2D-Diffusion	$[-\ln(1-\alpha)]^{-1}$	(1-α) ln(1-α) + α
4	3D-Diffusion	$3/2(1-\alpha)^{2/3}[1-(1-\alpha)^{1/3}]^{-1}$	$[1-(1-\alpha)^{1/3}]^2$
5	Avrami Erofeev	$3(1-\alpha)[-\ln(1-\alpha)]^{2/3}$	$[-\ln(1-\alpha)]^{1/3}$
6	Contracting Cylinder	$2(1-\alpha)^{1/2}$	$1-(1-\alpha)^{1/2}$

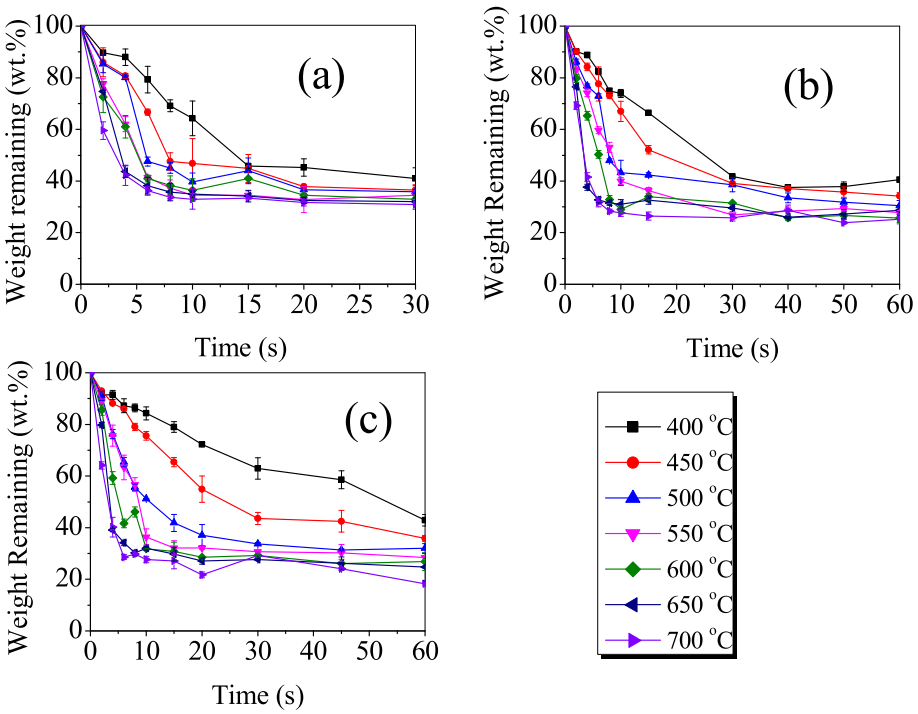

Fig. 1. Isothermal mass loss profiles of (a) RS, (b) PW and (c) EFB at various temperatures (400–700 °C) and hold times (2, 4, 6, 8, 10, 12, 14, 16, 18, 20, 30 and 60 s).

Table 4
Bio-chemical composition of RS, PW and EFB [31-33].

Biomass	RS	PW	EFB
Cellulose	32.1	40.0	37.3
Hemicellulose	28.0	26.9	14.6
Lignin	19.6	27.7	31.7
Ash/Others	20.3	5.0	16.4

the thermal degradation of high-ash materials are not very sensitive to the temperature. A study by Wang et al.[37] indicated that the presense of SiO_2 and other metallic components improves the intraparticle heat transfer, which accelerates the degradation at the interior of the particle. They also pointed out that, if the metals are not uniformly distributed within the particle, random nucleation centers are formed as the pyrolysis temperature increases.

The apparent activation energy and pre-exponential factor values vary in large range based on the experimental methodology and calculation techniques employed. For example, the activation energy for rice straw reported in two separate studies are 26.1 kJ/mol and 176.2 kJ/mol [38–40]. While the activation energy and pre-exponential factor values estimated using different techniques vary widely, the variation can be plotted on a single scale, which is based on 'kinetic compensation effect'. The kinetic compensation plot relates the apparent activation energy with the logarithm of the pre-exponential factor; $ln(k_0) = a \times E_a + b$[41-43]. In the expression, a and b are model-free parameters, also called as kinetic compensation parameters. The kinetic compensation plots for EFB, PW, and RS are depicted in Fig. 2.

The kinetic compensation effect is based on the assumption that the increase in the activation energy is accompanied by a corresponding increase in the pre-exponential factor and *vice versa*. Importantly, a number of experimental data points are taken from the literature that correspond to EFB, PW, and RS at slow heating conditions [25,26,44-58]. A majority of the (E_a, k_0) data sets corresponding to literature were determined by (a) fitting a first-order or nth order kinetic model to dynamic TG mass loss profiles, (b) fitting a distributed activation energy model with pseudo-components, (c) using single heating rate method of Coats-Redfern, and (d) using multiple heating rate method of Kissinger and Ozawa. The kinetic compensation expressions were found to be $ln(k_0) = 0.2E_a - 5.33$, $ln(k_0) = 0.2E_a - 3.90$ and $ln(k_0) = 0.088E_a - 2.51$ for EFB, PW and RS, respectively.

3.2. Time scale of fast pyrolysis of biomass

Fig. 3 depict the FTIR spectra of pyrolysates evolved from fast pyrolysis of EFB at 500 °C. The major functional group vibrations detected include: O–H stretch (3400 cm^{-1}), C–H aromatic stretch (3072 cm^{-1}) and methyl stretch (2962 cm^{-1}), $–CH_2–$ stretch of hydrocarbon

Table 5
List of kinetic parameters determined for fast pyrolysis of EFB, PW and RS.

	RS			PW			EFB		
Model	E_a	k_0	R^2	E_a	k_0	R^2	E_a	k_0	R^2
First order	18.5	4.1	0.99	37.1	26.5	0.97	34.3	28.1	0.96
1D-diffusion	21.7	1.8	0.98	39.7	14.8	0.97	34.6	9.5	0.98
2D-diffusion	28.7	4.1	0.95	44.7	26.1	0.96	38.7	13.3	0.96
3D-diffusion	13.0	0.2	0.94	49.4	20.3	0.96	48.9	24.5	0.96
Contracting cylinder	20.5	1.4	0.99	35.3	8.4	0.98	34.7	8.5	0.98
Avrami Erofeev	10.8	0.7	0.88	24.1	3.0	0.97	21.3	2.8	0.98

E_a and k_0 represent activation energy (kJ/mol) and pre-exponential factor (s^{-1}), respectively.

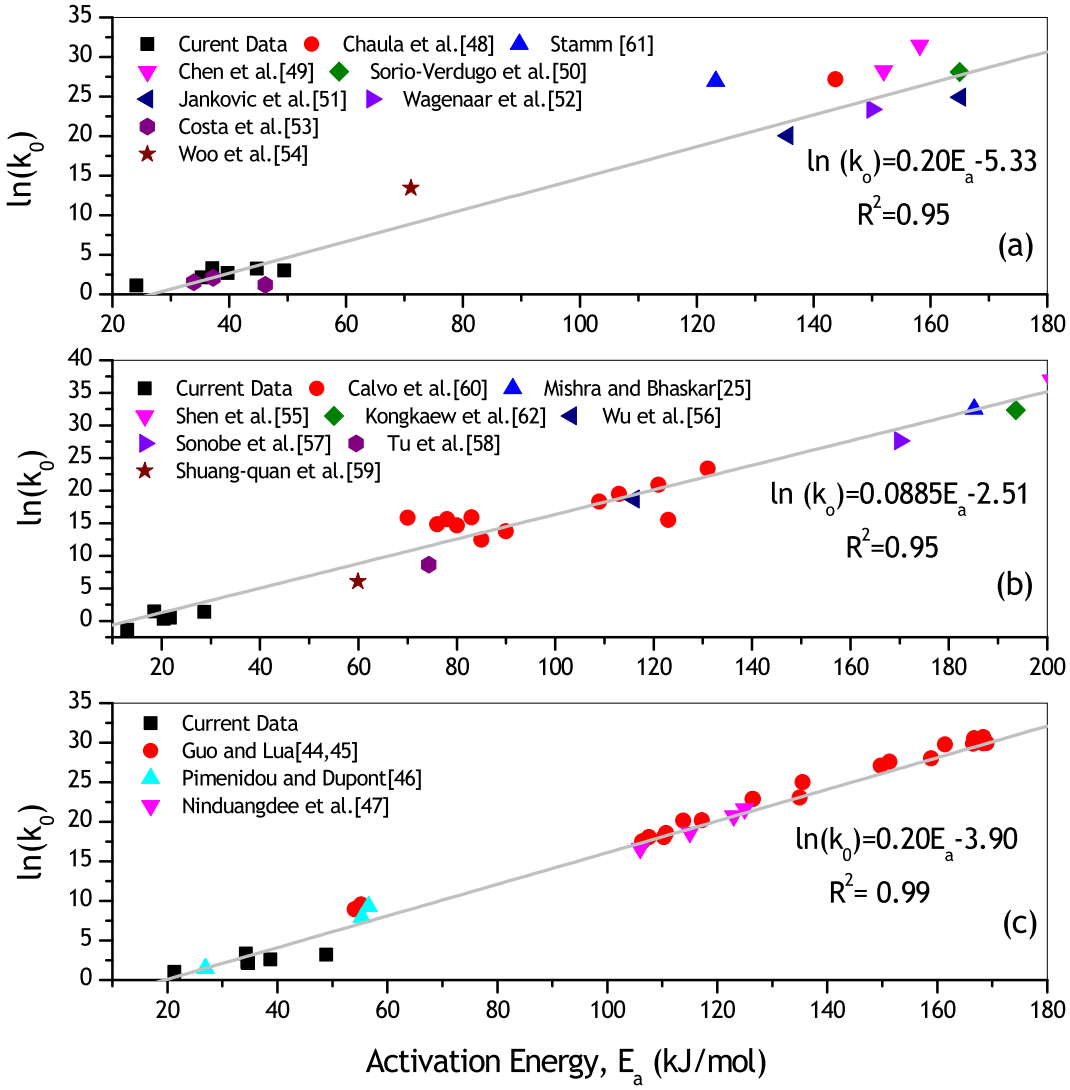

Fig. 2. Kinetic compensation plots for pyrolysis of (a) PW, (b) RS and (c) EFB based on the rate parameter data from the literature and this study.

backbone (2920–2933 cm^{-1}), C = O carbonyl stretch in aldehydes and ketones (1735 cm^{-1}), aromatic ring stretch (1506, 1615 cm^{-1}), C–C skeletal vibration (1127 cm^{-1}), C–O primary alcohol stretch (1056 cm^{-1}) and CO_2 (2348 cm^{-1}). More spectra can be seen in supplementary information (Figure S21-S28). It is clear that the evolution of vapors begins after 5 s (red curve) and then it increases rapidly until 9–13 s, and the evolution culminates after 60 s.

To simplify the discussion and for a better understanding, we define 'time to reach maximum rate of evolution (TRMRE)', which basically defines the time each function group takes to reach its maximum production rate in a particular experiment. It is important to note that the TRMRE analysis is not totally quantitative and it is prone to vary with carrier gas flow rate and distance between sample and IR beam path. We negate the complication arised due to these two factors by maintaining the constant flow rate in all the experiments, and by fixing the position and alignment of the sample in the brill cell. It is worth mentioning that the TRMRE does not directly represent the reaction time scale but it may have significance very similar to the half-life of a chemical reaction. The half-life analysis is widely used in chemical engineering and other streams.

The TRMRE values corresponding to different functional groups are compared to understand the evolution pattern and time scale of various functional groups with respect to each other. We observed that the TRMRE is different for different functional groups; TRMRE of C-O-C (methoxy) and carbonyl groups in fast pyrolysis of EFB at 500 °C are 19 and 13 s respectively. The variation of TRMRE clearly indicates that fast pyrolysis in the Pyroprobe is not rapid and it takes around a minute to complete. It also explains that the cellulose and hemicellulose-derived products (carbonyls) are mostly released in high quantities in the intial stage of the pyrolysis, while the lignin-derived product (methoxy groups) are mostly released at the later stage.

Fast pyrolysis is known to complete within a few seconds and the relatively large vapor evolution time (60 s) in our experiments can be due to the transport limitations. There are two possible resistances to the vapor transport in our experiments and shown in Fig. 4. Firstly resistance to the transport of generated vapor through the bed of unreacted biomass and char (solid–gas interactions), and secondly, the resistance experienced by the products sneaking out through the glass wool and mixing with the carrier gas stream (gas-film resistance). The mode of transport in both these cases is purely diffusion. The effect of transport resistances is also evident from the activation energy calculation, because the diffusion-based models fit the experimental data well. It is also important to note that the smaller molecules can diffuse out faster than the bulkier molecules but given a very small distance each molecule has to travel before it gets detected; the effect of transport limitation on the time scale is assumed negligible.

Fig. 5 depicts the time evolution of pyrolysates from PW, EFB and RS at 500 °C. It is clear that C = O(carbonyl) is more pronounced in the

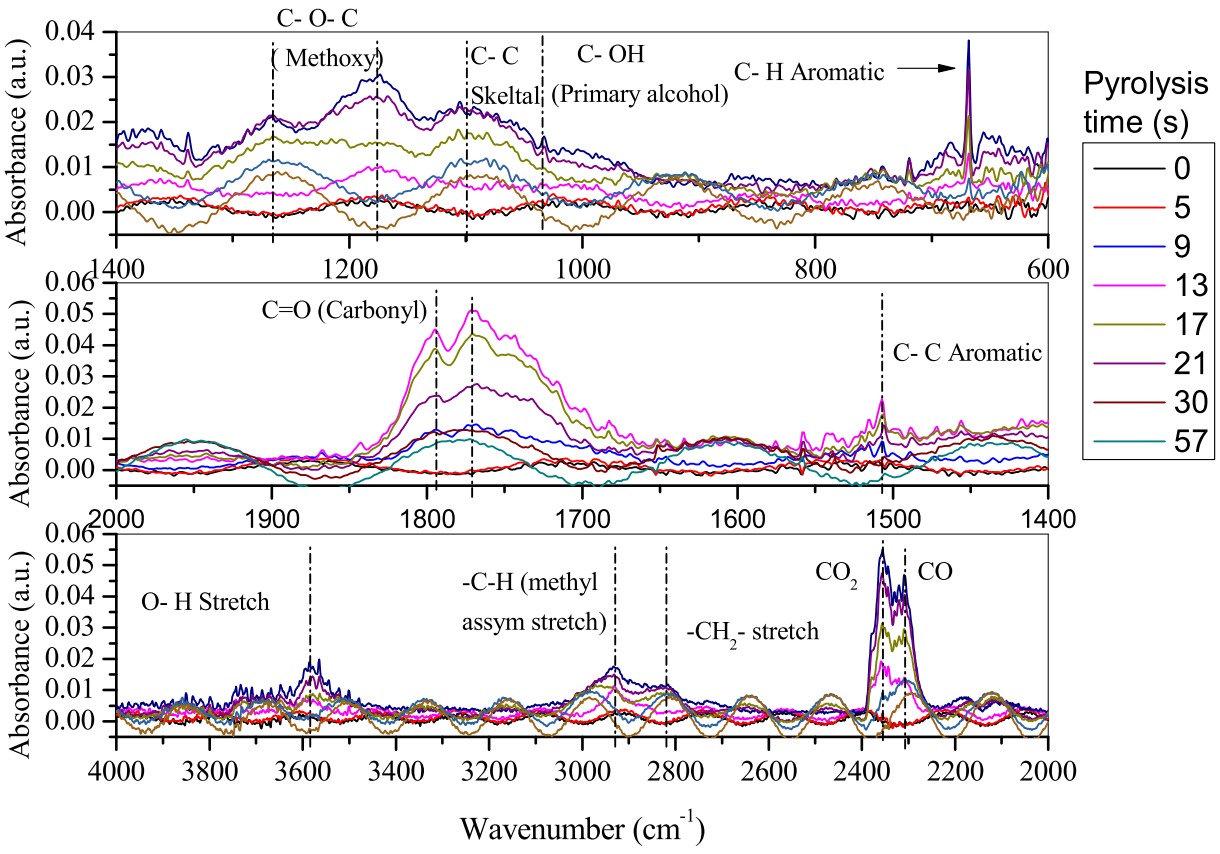

Fig. 3. Time evolution of FTIR spectra of pyrolysis vapors from fast pyrolysis of EFB at 500 °C.

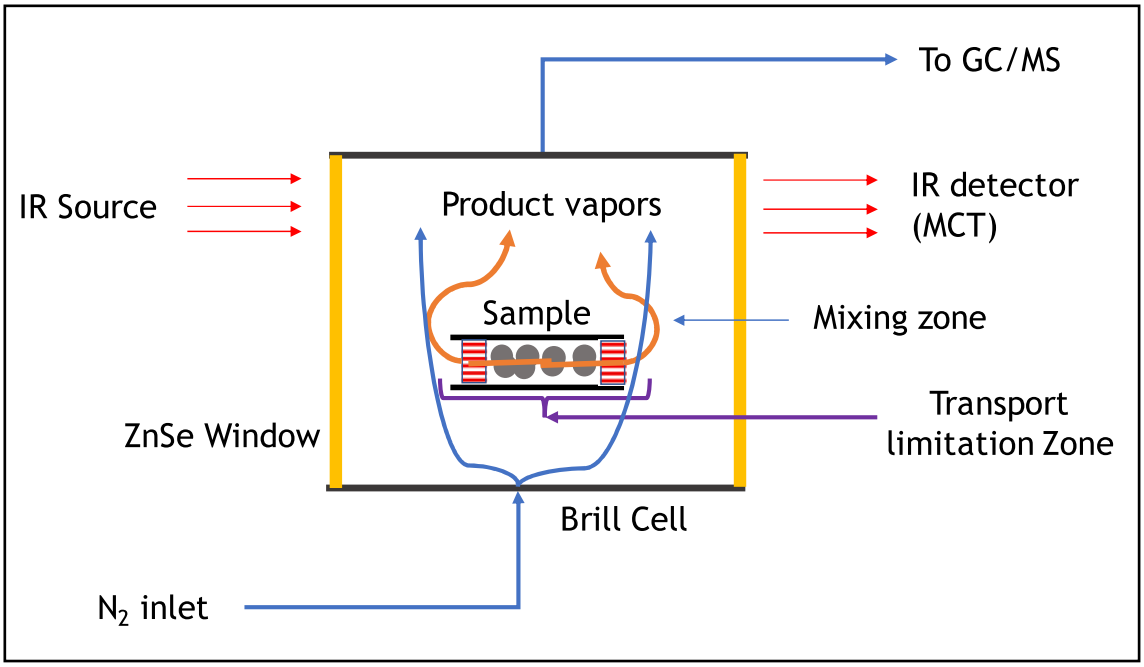

Fig. 4. Product vapor evolution and mass transfer zone in the Py-FTIR set-up.

pyrolysates from PW. The carbonyl groups are largly present in linear organics and carboxylic acids, which constitute the major fraction of the pyrolysates. The second most dominant funcational group is CO_2, which is generated from decarboxylation reaction. In EFB and RS, CO_2 is more prononounced followed by the C = O(carbonyl). The composition of various functional group is directly related to the type of biomass and pyrolysis conditions. However, the presence of ash alters the primary degradation pathway. Clearly CO_2 formation via decarboxylation and condensation reaction is promoted by the ash present in the biomass. As TRMRE is not a quantitative metric, the product formation will be

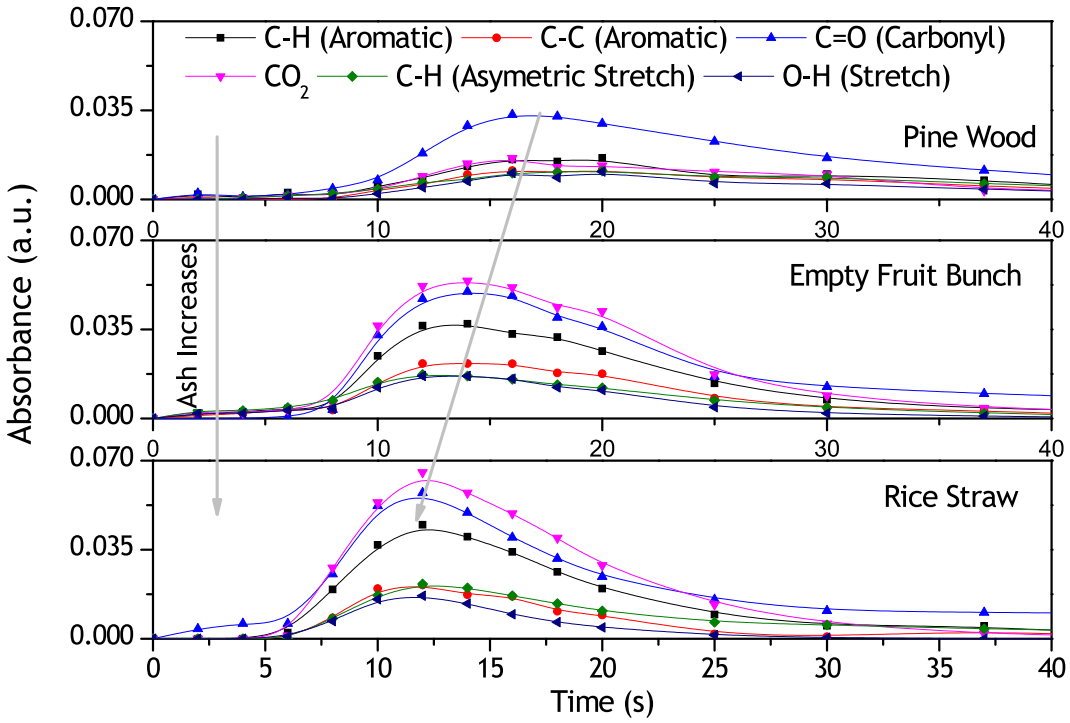

Fig. 5. Time evolution of major functional groups from fast pyrolysis of PW, EFB, and RS at 500 °C.

discussed in the next section.

It is interesting to note that the TRMRE values for three biomass follow the trend PW > EFB > RS. The variation of TRMRE is generally percieved to be directly linked with the amount of cellulose, hemicellulose and lignin in the biomass; higher the lignin or fixed carbon content, higher is the TRMRE. PW and EFB have very similar fixed carbon content but their TRMRE values are very different. This can be attributed, at least partially, to the affect of ash, because the TRMRE values follow a trend with ash content in biomass. TRMRE decreases with increase in ash in biomass as shown in Fig. 5. In the previous section, we discussed the formation of multiple nucleation centers because of non-uniform distribution of ash in the biomass. The nucleation centers catalyze the pyrolysis process by improving the heat transfer and/or by catalyzing the secondary decomposition of pyrolysis vapors. While the role of inert materials on heat tranfer improvement during biomass pyrolysis has not been studied very well, the catalytic effect of SiO_2 and Al_2O_3 in the C–C and C-O bond activation is well studied and reported [59-63]. Ash promotes the formation of non-condensable gasses and

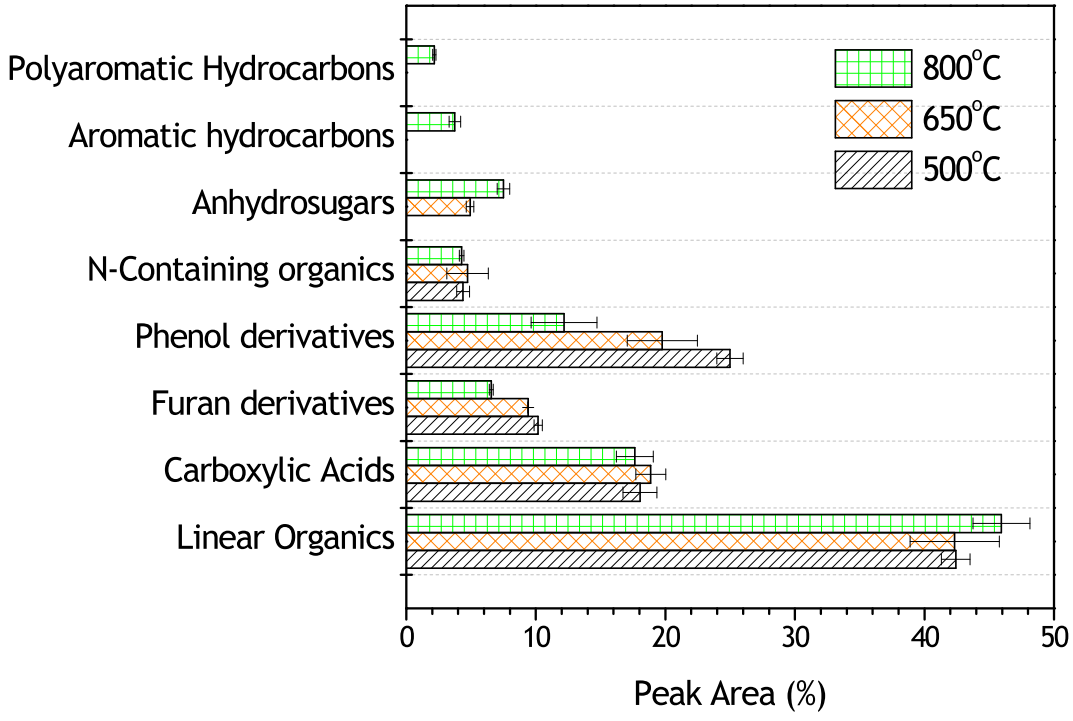

Fig. 6. Effect of temperature on the composition of pyrolysates from fast pyrolysis of PW.

char by cracking the larger molecules from the vapor and tar [63]. It also promotoes the condensation of the cracked vapors on the char surface.

3.3. Product composition from the fast pyrolysis of biomass

To evaluate the composition of the pyrolysates, fast pyrolysis experiments were conducted at various temperatures 500, 650, and 800 °C in the analytical Py-GC/MS set-up. The major product groups are depicted in Fig. 6, 7 and 8. Additionally, the details of all the products detected in fast pyrolysis can be found in Tables S1-S3 (Supplementary Information). The composition of the products is presented as relative peak area %. For simplicity in presentation, the products are grouped into eight distnict categories, viz. Aldehyde/ketones, carboxylic acids, furan derivatives, phenol derivatives, N-containing organics, anhydrosugars, aromatic hydrocarbons and polyaromatic hydrocarbons. It is observed that linear organics were the major products from fast pyrolysis of PW and RS, while carboxylic acid was the major product from the EFB at 500 °C.

It is interesting to note that acetic acid, which is one of the major pyrolysis products from hemicellulose, was observed in high yields from RS and EFB. The production of furan derivative was more from RS and PW, while it was less than 5% in EFB. As expected, a high production of phenolics especially guaiacol and methyl guaiacol was observed from both the lignin-rich woody biomass feedstock, viz., EFB and PW. The formation of aromatic hydrocarbons were not observed from any biomass at 500 °C.

The effect of ash was more pronounced on the activation energy calculation and the time scale of fast pyrolysis. However, no-specific effect of ash was observed on the liquid product composition at 500 °C. This may be due to the fact that ash is primarily responsible for catalyzing the condensation reactions, which leads to the formation of high molecular weight products similar to coke. Temperature has a conspicuous effect on the formation of major products. It is observed that the total selectivity of linear organics decreases with increase in temperature for RS and EFB. In contrast, the selectivity of linear organics increases for PW when temperature increased from 500 to 800 °C. Interestingly, as we move to higher temperatures, the selectivity of phenol derivatives decreases significantly for PW, while there was no significant variation observed for RS and EFB.

From the above discussion, it is inferred that the effect of temperature is not uniform on all biomass types. The ash content may have an important role on product formation, particularly at high temperatures. The conversion of phenol derivatives to aromatic hydrocarbons via C-O bond scission is known to occur at high temperatures (>600 °C). Most of the phenolics in PW converted to aromatic and polyaromatic hydrocarbons at 800 °C. However, for high-ash biomass such as RS, significant production of aromatics is observed, without any reduction in phenol derivatives. Two possibilities exist: (a) there should be an alternative route for aromatic hydrocarbons production which does not involve phenolics, (b) there should be another route to form phenolics to compensate for the quantity of phenolics which is converted to the aromatic hydrocarbons. The latter possibility is likely to be more realistic as the reduction in yield of furan derivatives and linear organics is observed at 800 °C. The SiO_2-rich ash of RS seems to catalyze the condensation of furan derivatives and linear organicsto produce phenolics.

Alternatively, the reduction in total phenolics production from low ash biomass such as PW can be attributed to the formation of aromatic hydrocarbons via cleavage of hydroxyl and methoxy linkages of guaiacol and other phenolic derivatives [13,31]. The cleaved propyl side chains of the C9 monomers of lignin and other methoxy phenols lead to the formation of aldehyde/ketones. From the structure of aromatic hydrocarbons produced, it can be inferred that the formation of benzene, toluene, and styrene proceeds via cleavage of methoxy and hydroxy linkages of phenol, guaiacol, and vinyl guaiacol [13,31]. Products such as cresol and methyl anisole are stable intermediates formed via cleavage of methoxy and hydroxy units of methyl guaiacol, respectively. The intermediates further transform to toluene, which is one of the major products at 800 °C.

3.4. Conclusion

In this study, kinetics of fast pyrolysis of EFB, PW, and RS was conducted using analytical Py-FTIR and Py-GC/MS set-ups. The mass loss profiles of biomass were generated at different temperatures and using empirical models, the apparent kinetic parameters were determined. Kinetic compensation plot was constructed to validate the variation of apparent activation energy with pre-exponential factor. The time evolution of the vapor products were analyzed and 'time to reach maximum rate of evolution' followed the trend: PW > EFB > RS. The fast pyrolysis

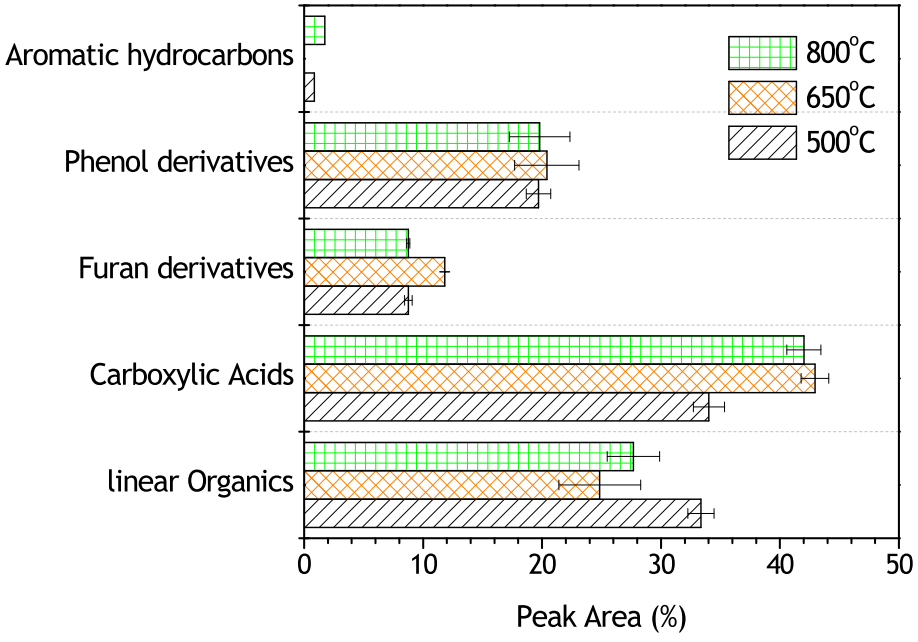

Fig. 7. Effect of temperature on the composition of pyrolysates from fast pyrolysis of EFB.

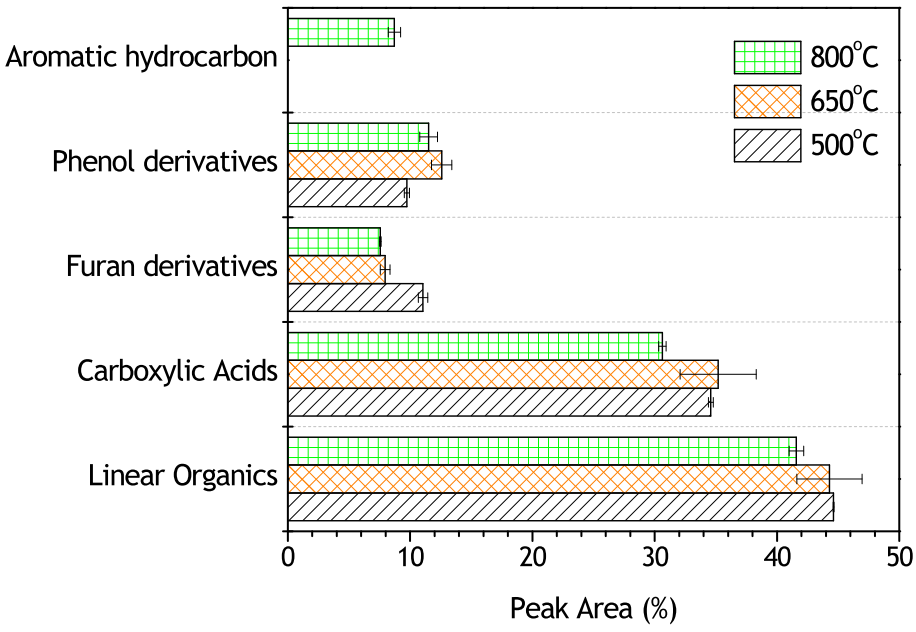

Fig. 8. Effect of temperature on the composition of pyrolysates from fast pyrolysis of RS.

products were analyzed using online GC/MS and effect of biomass constituent and ash was highlighted. PW and EFB resulted in more phenol derivativaes while RS yielded more linear organics.

Declaration of Competing Interest

The authors declare that they have no known competing financial interests or personal relationships that could have appeared to influence the work reported in this paper.

Acknowledgement

The National Center for Combustion Research and Development is sponsored by the Department of Science and Technology (DST), India. The authors also thank Valmet Technologies Pvt. Ltd. Chennai, for partially funding this study.

Appendix A. Supplementary data

Supplementary data to this article can be found online at https://doi.org/10.1016/j.ecmx.2020.100071.

References

[1] Kohli K, Prajapati R, Sharma BK. Bio-based chemicals from renewable biomass for integrated biorefineries. Energies 2019;12:233–73.
[2] Uzoejinwa BB, He X, Wang S, El-Fatah Abomohra A, Hu Y, Wang Q. Co-pyrolysis of biomass and waste plastics as a thermochemical conversion technology for high-grade biofuel production: Recent progress and future directions elsewhere worldwide. Energy Convers Manage 2018;163:468–92. https://doi.org/10.1016/j.enconman.2018.02.004.
[3] Bridgwater AV. Review of fast pyrolysis of biomass and product upgrading. Biomass Bioenergy 2012;38:68–94. https://doi.org/10.1016/j.biombioe.2011.01.048.
[4] Kanaujia PK, Sharma YK, Garg MO, Tripathi D, Singh R. Review of analytical strategies in the production and upgrading of bio-oils derived from lignocellulosic biomass. J Anal App pyrol 2014;105:55–74.
[5] Patwardhan PR, Satrio JA, Brown RC, Shanks BH. Product distribution from fast pyrolysis of glucose-based carbohydrates. J Anal Appl Pyrol 2009;86:323–30.
[6] Patwardhan PR, Brown RC, Shanks BH. Understanding the Fast Pyrolysis of Lignin. ChemSusChem 2011;4(11):1629–36. https://doi.org/10.1002/cssc.201100133.
[7] Newalkar G, Iisa K, D'Amico AD, Sievers C, Agrawal P. Effect of temperature, pressure, and residence time on pyrolysis of pine in an entrained flow reactor. Energy Fuels 2014;28(8):5144–57. https://doi.org/10.1021/ef5009715.
[8] Hernández MA, García ÁN, Gómez A, Agulló J, Marcilla A. Effect of residence time on volatile products obtained in the HDPE pyrolysis in the presence and absence of HZSm-5. Ind Eng Chem Res 2006;45:8770–8.
[9] Gomez N, Banks SW, Nowakowski DJ, Rosas JG, Cara J, Sanchez ME, et al. Effect of temperature on product performance of a high ash biomass during fast pyrolysis and its bio-oil storage evaluation. Fuel Proc Technol 2018;171:97–105.
[10] Krumm C, Pfaendtner J, Dauenhauer PJ. Millisecond pulsed film unify the mechanism of cellulose fragmentation. ACS Chem Mat 2016;28:3108–14.
[11] Maduskar S, Facas GG, Papageorgiou C, Williams CL, Dauenhauer PJ. Five rules for measuring biomass pyrolysis rates: Pulse-heated analysis of solid reaction kinetics of lignocellulosic biomass. ACS Sust Chem Eng 2018;6:1387–99.
[12] Vinu R, Broadbelt LJ. A mechanistic model of fast pyrolysis of glucose-based carbohydrates to predict bio-oil composition. Energy Environ Sci 2012;5:9808–26.
[13] Ojha DK, Viju D, Vinu R. Fast pyrolysis kinetics of alkali lignin: Evolution of apparent rate parameters and product time evolution. Bioresour Technol 2017;241:142–51.
[14] Apaydin-Varol E, Uzun BB, Önal E, Pütün AE. Synthetic fuel production from cottonseed: Fast pyrolysis and a TGA/FT-IR/MS study. J Anal Appl Pyrol 2014;105:83–90.
[15] Shen DK, Gu S. The mechanism for thermal decomposition of cellulose and its main products. Bioresour Technol 2009;100:6496–504.
[16] Li S, Lyons-Hart J, Banyasz J, Shafer K. Real-time evolved gas analysis by FTIR method: an experimental study of cellulose pyrolysis. Fuel 2001;80(12):1809–17. https://doi.org/10.1016/S0016-2361(01)00064-3.
[17] Liu Q, Zhong Z, Wang S, Luo Z. Interaction of biomass components during pyrolysis: A TG- FTIR study. J Anal Appl Pyrol 2011;90:213–8.
[18] Salema AA, Afzal MT, Motasemi F. Is there a synergy between carbonaceous material and biomass during conventional pyrolysis? A TG- FTIR approach. J Anal Appl Pyrol 2014;105:217–26.
[19] Ojha DK, Vinu R. Fast co-pyrolysis of cellulose and polypropylene using Py- GC/MS and Py- FT-IR. RSC Adv 2015;5:66861–70.
[20] Ojha DK, Shukla S, Sachin RS, Vinu R. Understanding the interactions between cellulose and polypropylene during fast co-pyrolysis via experiments and DFT calculations. Chem Eng Trans 2016;50:67–72.
[21] Vyazovkin S, Burnham AK, Criado JM, Pérez-Maqueda LA, Popescu C, Sbirrazzuoli N. ICTAC kinetic committee recommendations for performing kinetic computations on thermal analysis data. Thermochim Acta 2011;520:1–19.
[22] Ozsin G, Putun AE. Insight into pyrolysis and co-pyrolysis of biomass and polystyrene: Thermochemical behaviors, kinetics and evolved gas analysis. Energy Conver Manage 2017;149:675–85.
[23] Ozsin G, Putun AE. TGA/MS/FT-IR study for kinetic evolution and evolved gas analysis of a biomass/PVC co-pyrolysis process. Energy Conver Manage 2019;182:143–53.
[24] Liu H, Ahmad MS, Alhumade H, Elkamel A, Sanmak S, Shen B. Energy Conver. Manage 2020;208:1–11.
[25] Mishra G, Bhaskar T. Non isothermal model free kinetics for pyrolysis of rice straw. Bioresour Technol 2014;169:614–21. https://doi.org/10.1016/j.biortech.2014.07.045.
[26] Wu Q, Yao F, Xu X, Mei C, Zhou D. Thermal degradation of rice straw fibers: global kinetic modeling with isothermal thermogravimetric analysis. J Ind Eng Chem 2013;19:670–6.

[27] Soria- Verdugo A, Goos E, García-Hernando N. Effect of the number of TGA curves employed on the biomass pyrolysis kinetics results obtained using the Distributed Activation Energy Model. Fuel Process Technol 2015;134:360–71.
[28] Vassilev SV, Baxter D, Andersen LK, Vassileva CC. An overview of the chemical composition of biomass. Fuel 2010;89:913–33.
[29] Bhargava R, Levin IW. Gram-Schmidt orthogonalization for rapid reconstructions of Fourier transform infrared spectroscopic imaging data. Appl Spectrosc 2004;58 (8):995–1000.
[30] Ranzi E, Cuoci A, Faravelli T, Frassoldati A, Migliavacca G, Pierucci S, et al. Chemical kinetics of biomass pyrolysis. Energy Fuels 2008;22:4292–300.
[31] Shawky BT, Mahmoud MG, Ghazy EA, Asker MHS, Ibrahim GS. Enzymatic hydrolysis of rice straw and corn stalks for monosugars production. J Gen Eng Biotech 2011;9:59–63.
[32] Sjostrom E, Chemistry W. Fundamentals and Applications. second ed. San Diego: Academic Press; 1993. p. 292.
[33] Sudiyani Y, Styarini D, Triwahyuni E, Sudiyarmanto, Sembiring KC, Aristiawan Y, Abimanyu H, Han MH. Utilization of biomass waste empty fruit bunch fiber of palm oil for bioethanol production using pilot scale unit. Energ Proced 2013;32: 31–8.
[34] Calonaci M, Grana R, Hemings EB, Bozzano G, Dente M, Ranzi E. Comprehensive kinetic modeling study of bio-oil formation from fast pyrolysis of biomass. Energy Fuels 2010;24:5727–34.
[35] Zhao J, Xiuwen W, Hu J, Liu Q, Shen D, Xiao R. Thermal degradation of softwood lignin by TG- FTIR and Py- GC/MS. Polym Degrad Stabil 2014;108:133–8.
[36] Fogler, H.S. Elements of chemical reaction engineering, 3rd Edition, 753-754.
[37] Wang Q, Endo T, Apar P, Gui L, Chen Q, Mitsumura N, Qian Q, Niida H, Animesh S, Sekiguchi K. Study on hetrogeneous reaction between tar and ash from waste biomass pyrolysis and gassification. WIT Trans Ecol Envir 2013;176:291–302. https://doi.org/10.2495/ESUS130251.
[38] Demirbaş A. Relationship between heating value and lignin, fixed carbon and volatile material contents of shells from biomass products. Energy Sources 2003; 25:629–35.
[39] Tora EA, Adwan AM, Hamad MA. Kinetics of thermal decomposition of Egyptian cotton stalks, corn stalks and rice straw. ARPN J Eng Appl Sci 2016;11:1–9.
[40] Yao F, Wu Q, Lei Y, Guo W, Xu Y. Thermal decomposition kinetics of natural fibers: Activation energy with dynamic thermogravimetric analysis. Polym Degrad Stabil 2008;93:90–8.
[41] Agrawal RK. On the compensation effect. J Therm Anal 1986;31:73–86.
[42] Zsakó J. The kinetic compensation effect. J Therm Anal Calorim 1976;9:101–8.
[43] Garn Paul D. Kinetics of thermal decomposition of the solid state. Thermochim Acta 1990;160(2):135–45. https://doi.org/10.1016/0040-6031(90)80254-V.
[44] Guo J, Lua AC. Kinetic study on pyrolysis of extracted oil palm fiber. J Therm Anal Calorim 2000;59:763–74.
[45] Guo J, Lua AC. Kinetic study on the pyrolytic process of oil-palm solid waste using two-step consecutive reaction model. Biomass Bioenergy 2001;20:223–33.
[46] Pimenidou P, Dupont V. Characterization of palm empty fruit bunch (PEFB) and pinewood bio-oils and kinetics of their thermal degradation. Bioresour Technol 2012;109:198–205.
[47] Ninduangdee P, Kuprianov VI, Cha EY, Kaewrath R, Youngyuen P, Atthawethworawuth W. Thermogravimetric studies of oil palm empty fruit bunch and palm kernel shell: TG/DTG analysis and modeling. Energy Procedia 2015;79: 453–8.
[48] Chaula Z, Said M, John G. Thermal characterization of pine sawdust as energy source feedstock. J Energy Technol Policy 2014;4:57–64.
[49] Chen Z, Hu M, Zhu X, Guo D, Liu S, Hu Z, et al. Characterization and kinetic study on pyrolysis of five lignocellulosic biomass via thermogravimetric analysis. Bioresour Technol 2015;192:441–50.
[50] Sorio-Verdugo A, Goos E, García-Hernando N. Effect of the number of TGA curves employed on the biomass pyrolysis kinetics results obtained using the distributed activation energy model. Fuel Process Technol 2015;134:360–71.
[51] Janković BŽ, Janković MM. Pyrolysis of pine and beech wood under isothermal conditions: the conventional kinetic approach. Res Chem Intermed 2015;41: 2201–19.
[52] Wagenaar BM, Prins W, van Swaaij WPM. Flash pyrolysis kinetics of pinewood. Fuel Process Technol 1993;36:291–8.
[53] Costa VJ, Vieira RM, Girotto SBFT, Simioni FJ. Pyrolysis and thermogravimetry of blended and nonblended residues of pine and eucalyptus forestry woods. Environ Progress Sustain Energy 2016;35:1521–8.
[54] Woo JK, Schniewind AP. Thermal degradation of wood treated with fire retardants. Holzforschung 1987;41:305–13.
[55] Sheng J, Ji D, Yu F, Cui L, Zeng Q, Ai N, et al. Influence of chemical treatment on rice straw pyrolysis by TG-FTIR. IERI Procedia 2014;8:30–4.
[56] Sonobe, T.; Pipatmanomai, S.; Worasuwannarak, N. Pyrolysis characteristics of Thai-agricultural residues of rice straw, rice husk, and corncob by TG-MS technique and kinetic analysis, The 2nd joint international conference on "Sustainable Energy and Environment (SEE 2006)" 21-23 November 2006, Bangkok, Thailand.
[57] Tu W-K, Shie J-L, Chang C-Y, Chang C-F, Lin C-F, Yang S-Y, et al. Products and bioenergy from the pyrolysis of rice straw via radio frequency plasma and its kinetics. Bioresour Technol 2009;100:2052–61.
[58] Shuang-Quan Z, Xiao-ming Y, Zhi-yuan Y, Ting-ting P, Ming-Jian D, Tian-yu S. Study of the co-pyrolysis behavior of sewage-sludge/rice-straw and the kinetics. Procedia Earth Planetary Sci 2009;1:661–6.
[59] Calvo LF, Otero M, Jenkins BM, Morán A, García AI. Heating process characteristics and kinetics of rice straw in a different atmosphere. Fuel Process Technol 2004;85:279–91.
[60] Stamm A. Thermal degradation of wood and cellulose. Ind Eng Chem 1956;48: 413–7.
[61] Kongkaew N, Pruksakit W, Patumsawad S. Thermogravimetric kinetic analysis of the pyrolysis of rice straw. Energy Procedia 2015;79:663–70.
[62] Ramos-Fernández EV, Ruiz-Martínez J, Serrano-Ruiz JC, Silvestre-Albero J, Sepúlveda-Escribano A, Rodríguez-Reinoso F. Effect of the support, Al_2O_3 or SiO_2 on the catalytic behavior of Cr-ZnO promoted Pt catalysts in the selective hydrogenation of cinnamaldehyde. Appl Catal A: Gen 2011;402:50–8.
[63] Yildiz G, Ronsse F, Venderbosch R, Duren RV, Kersten SRA, Prins W. Effect of biomass ash in catalytic fast pyrolysis of pine wood. Appl Catal B: Env 2015; 168–169:203–11.